Calhoun: The NPS Institutional Archive

DSpace Repository

Faculty and Researchers | Faculty and Researchers' Publications

1991

Stator Averaged, Rotor Blade-to-Blade near Wall Flow in a Multistage Axial Compressor with Tip Clearance Variation

Moyle, I.N.; Walker, G.J.; Shreeve, R.P.

ASME

Moyle, I. N., G. J. Walker, and R. P. Shreeve. "Stator Averaged, Rotor Blade-to-Blade Near Wall Flow in a Multistage Axial Compressor With Tip Clearance Variation." ASME 1991 International Gas Turbine and Aeroengine Congress and Exposition. American Society of Mechanical Engineers, 1991.

http://hdl.handle.net/10945/61952

This publication is a work of the U.S. Government as defined in Title 17, United States Code, Section 101. Copyright protection is not available for this work in the United States.

Downloaded from NPS Archive: Calhoun

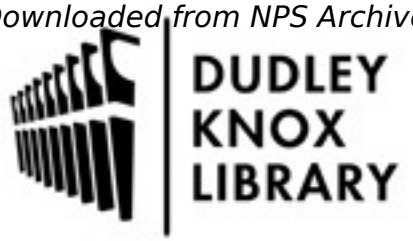

http://www.nps.edu/library

Calhoun is the Naval Postgraduate School's public access digital repository for research materials and institutional publications created by the NPS community. Calhoun is named for Professor of Mathematics Guy K. Calhoun, NPS's first appointed -- and published -- scholarly author.

Dudley Knox Library / Naval Postgraduate School
411 Dyer Road / 1 University Circle
Monterey, California USA 93943

THE AMERICAN SOCIETY OF MECHANICAL ENGINEERS
345 E. 47 St., New York, N.Y. 10017

91-GT-30

The Society shall not be responsible for statements or opinions advanced in papers or in discussion at meetings of the Society or of its Divisions or Sections, or printed in its publications. Discussion is printed only if the paper is published in an ASME Journal. Papers are available from ASME for fifteen months after the meeting.
Printed in USA.

Copyright © 1991 by ASME

Stator Averaged, Rotor Blade-to-Blade Near Wall Flow in a Multistage Axial Compressor with Tip Clearance Variation

I. N. MOYLE[1], G. J. WALKER[2] and R. P. SHREEVE
Turbopropulsion Laboratory
Naval Postgraduate School
Monterey, California 93943

Abstract

This paper describes the effect of tip clearance changes on the pressure at the case wall of a second stage rotor. Wall shear distributions under the rotor tip are also presented. The results show low pressure areas extending along the rotor suction side but lying away from the blade. Pressure contours indicate the tangential loading at the tip is lower than predicted by two dimensional calculations, however, the predicted loading is observed between the lowest pressure's path in the passage and the blade pressure side. The results suggest a viscous or shearing layer, due to blade-to-wall relative motion, is generated on the blade side of the tip gap which modifies the inviscid relative flow field and produces an unloading on the blade tip.

Nomenclature

b	blade height
c	blade chord
Cp	pressure coefficient, (p-pref)/(0.5ρUt^2)
e	clearance gap
p	static pressure
r	radius
Ru	Reynolds Number, ρcUt/μ
t	maximum blade element thickness
U	blade tangential or whirl velocity
W	relative velocity
Φ	passage average flow coefficient, Va/Ut
Ω	rotor angular velocity
ξ	blade element camber
γ	blade element stagger

Subscripts

t	at tip radius

[1] Lockheed Missiles and Space Company, California
[2] University of Tasmania, Australia

INTRODUCTION

Selected results from a program of flow measurements conducted in a low speed multistage axial compressor at the Naval Postgraduate School are presented. The objective of the program was to examine the effects of tip clearance changes on axial compressor performance.

Case wall conditions were surveyed at gap-to-blade height ratios (e/b) of 0.0035 and 0.006 in a casing that was 0.0002 of blade height out of round. The flow for these clearances was measured at peak power input, near design and at an open throttle condition on a constant speed throttle line. The flow was also examined with a rubbing seal on the pressure side of one blade for the design flow coefficient.

APPARATUS AND MEASUREMENTS

The compressor test section had a tip radius of 457 mm (18 in) and a hub-to-tip ratio of 0.6. For the experiments described the test section was fitted with an inlet guide vane row of 30 blades, two 30 rotor / 32 stator stages in the second and third stage positions and a 30 blade exit guide vane row in the first exit position, Figure 1. The first stage position was not bladed to allow survey access upstream of the rotor. The compressor rotational speed was 1610 RPM with a tip speed of 77.08 m/s (252.9 ft/s). Screens or plates of different flow resistance were placed in a throttle housing two duct diameters upstream of the test section to vary the air flow rate.

Stage Design The blade whirl distribution was of the solid body type and the velocity diagram was symmetric. Profiles for the rotor and stator were developed from a circular arc camber line and a modified C-4 thickness distribution. The thickness distribution was slightly flattened at the leading edge. The blading geometry is set out in Table 1. The design is described in detail in Vavra (1973). The Reynolds Number (Ru) was 4.2x10^5 at the tip for the design flow condition.

Presented at the International Gas Turbine and Aeroengine Congress and Exposition
Orlando, FL June 3-6, 1991
This paper has been accepted for publication in the Transactions of the ASME
Discussion of it will be accepted at ASME Headquarters until September 30, 1991

Downloaded From: https://proceedings.asmedigitalcollection.asme.org on 04/08/2019 Terms of Use: http://www.asme.org/about-asme/terms-of-use

Table 1

Spanwise Distribution of Blading Geometric Design Data; b = 183 mm (7.20 in).

Rotor				
r/rt	γ	ξ	c/b	t/c
(-)	(°)	(°)	(-)	(-)
0.60	15.71	40.48	.333	.125
0.70	20.30	37.42	.361	.098
0.80	25.56	32.54	.389	.076
0.90	32.19	26.34	.417	.068
1.00	40.96	16.00	.444	.062

Stator				
r/rt	γ	ξ	c/b	t/c
(-)	(°)	(°)	(-)	(-)
0.60	16.07	29.26	.361	.065
0.70	21.10	29.28	.347	.076
0.80	26.21	31.44	.333	.087
0.90	31.20	36.91	.319	.100
1.00	34.71	47.58	.306	.114

Blade-to-Blade Survey Procedure High frequency response sensors and a timing signal from the compressor shaft were used to measure the flow relative to the instantaneous position of the rotor blade. Based on the analysis of Moyle (1989a), flows very near the rotor suction and pressure sides at the tip were of particular interest in this study. Using the shaft signal to trigger a square wave generator which, in turn, triggered a stroboscope; an image of the blade tip was stopped in a window in the compressor case wall. By adjusting the square wave period, a scribed line on the tip could be placed under cross hairs on the window. The rotor tip was located to within 0.005 of the rotor blade spacing using this technique. The strobe trigger also started the data system, which was capable of sampling at intervals smaller than 0.001 of the blade spacing.

With the rotor position known, moving a sensor circumferentially relative to the upstream stator permitted stator relative quantity distributions to be determined in the rotor. Sensor data from many stator relative positions were combined to form rotor blade-to-blade averages. The resulting pressure distributions were compared with the predicted pressure field from quasi-three dimensional blade-to-blade flow calculations. A contoured plate fixture, which permitted these types of surveys and averaging, was developed for the compressor case. The plate design prevented leakage into the flow region being surveyed and is shown in Figure 2.

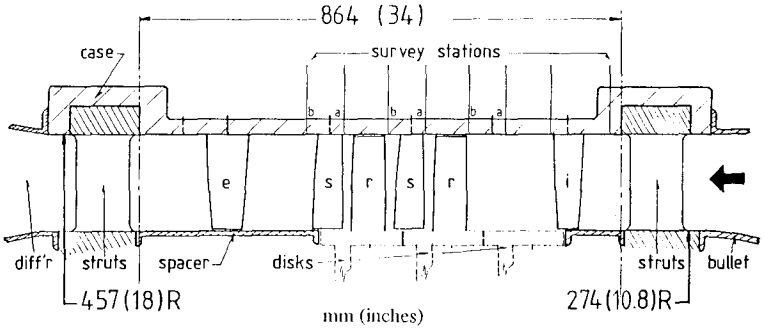

Fig. 1 Compressor test section for the two stage build.

Case Wall Static Pressure (WP) Surveys Static pressure distributions at the case wall, under and between the rotor blades, were acquired by moving a plug, fitted with a centrally located, flush mounted Kulite XCS-093-1D high response pressure transducer, to various hole locations on the wall plate discussed above. The plate, positioned flush with the wall above the second rotor, carried a matrix of six holes spanning the axial chord and five holes spanning one stator pitch circumferentially. The plate's position relative to the stator blades is shown in Figure 2.

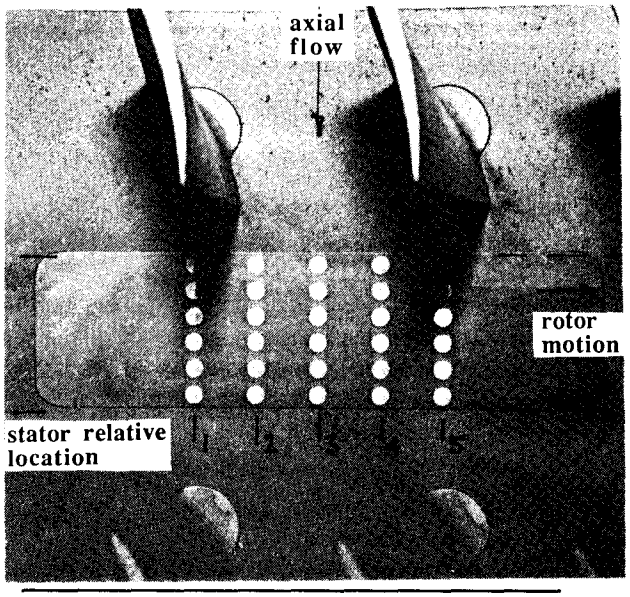

Fig. 2 Survey plate in the test section wall used for wall pressure and shear measurements under the rotor. The relative location of stator blades is shown with the rotor removed.

Downloaded From: https://proceedings.asmedigitalcollection.asme.org on 04/08/2019 Terms of Use: http://www.asme.org/about-asme/terms-of-use

One transducer measured all the wall pressure data presented. Systematic error in the data was minimized by having the same calibration and sensor characteristics for all the readings. As the measured flow was unsteady in the absolute frame, the unsteady response of the transducer was examined thoroughly to ensure that it was, in fact, tracking the unsteady wall pressure under the rotor path. Measurements of the same flow condition were made with different orientations of the probe, different depths of immersion and with selective covering of the sensor's protective screen. The output signal spectrum was found to be free of unacceptable resonances. The probe resolved to within 0.01 of spacing and had a frequency response of 100 kHz compared to the blade passing frequency of 805 Hz. Such resolution was more than adequate for interpretation of the results presented. The calibration, response and verification tests are described in detail in Moyle (1989b, Sec A.5).

Case Wall Skin Friction (WS) Surveys A skin friction sensor was developed by capping a high response pressure transducer (Kulite XCS-093-1D) with an abrupt, forward facing step fixed on the "M" screen over the sensing element, Figure 3. The step decelerated the flow near the wall to its stagnation pressure, which was detected by the sensor. The previously measured wall pressure was used as the pressure datum needed to determine the shear.

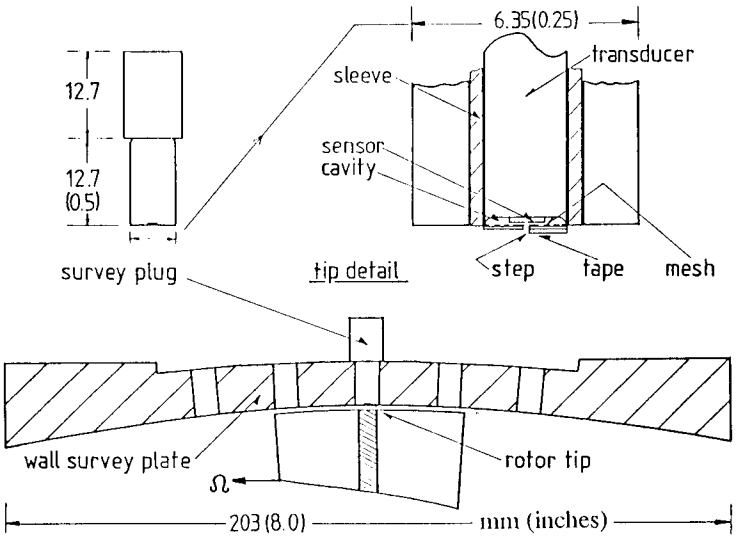

Fig. 3 Wall shear probe geometry and mounting in the wall plate.

Measurements at six yaw angles of the probe for each hole in the wall plate were used to resolve the direction and magnitude of the wall shear vector. Preliminary measurements using prototype hardware are presented. The verification processes for the prototype were similar to those applied for the wall pressure probe and are described in Moyle (1989b). A number of step heights were tried with consistent results and the WS probe's spatial resolution was better than the WP probe due to its smaller sensing area. The probe had an output of wall pressure at zero shear. This known calibration point proved to be the most significant in interpreting the flow conditions near the tip gap.

Data Acquisition and Reduction When acquiring data, the rotor blade spacing was sampled in increments of 1%. Two passages were routinely surveyed after confirming the periodicity from samples of three and five passages. Acquisition of blade-to-blade information resulted in voluminous quantities of data. Each of the six axial stations on the wall survey plate contained five peripheral holes for a total of (6 x 5 x 200 = 6000) wall pressure readings per survey and a matching 6000 standard deviation records. Interpolated data (from a row of six axial holes) were stored in (60 x 200) matrices for plotting and data reduction. When surfaces or contour maps are examined to resolve flow features smaller than one sixth of axial chord, it advisable to recall that the picture is based on interpolation of a 6 x 200 data point set.

A pressure coefficient (C_p), defined as the difference in wall pressure from a pressure datum divided by the wheel dynamic pressure at the tip ($0.5\rho U_t^2$), was used to normalize the data. A contour interval of 4% of C_p was used for plotting. This interval is equivalent to 6% of a C_p based on the tip relative velocity (Wt) of the velocity diagram at design conditions. The measurement uncertainty in C_p was less than 0.4%.

Test Conditions The throttle settings and clearances for the surveys are shown below in Table 2. The flow coefficients in the table reflect the following conditions; $\Phi = 0.64$ was the design flow coefficient, $\Phi = 0.60$ was slightly below maximum power input to the flow and $\Phi = 0.68$ was an open throttle condition. The flow coefficient was derived from test section mass flow, tip speed, compressor face density and test section area.

Table 2

Surveys taken in the Two Stage Build at Various Flow Coefficient Conditions; RS = Radial Interrow, WP = Wall Pressure, WS = Wall Shear

Clearance (e/b)	Φ	RS	WP	WS
0.0035	0.60		X	
	0.64	X	X	X
	0.68		X	
0.0060	0.60		X	
	0.64	X	X	
	0.68		X	

Downloaded From: https://proceedings.asmedigitalcollection.asme.org on 04/08/2019 Terms of Use: http://www.asme.org/about-asme/terms-of-use

FLOW IN THE TIP/WALL CORNER

Contours of pressure coefficient were found to exhibit distinct and consistent flow features over a wide range of conditions. The general flow structure near the blade tip and case wall corner was determined from the wall pressure distribution at *one clearance level* in a rotor passage (blades 2-3) over a range of flow conditions.

Basic Pressure Pattern (Stator Averaged) A surface view of such a distribution, Figure 4, shows the main features of the flow. The (leftmost) high pressure ridge corresponds to the position of the pressure side of rotor blade 2. The pressure magnitude was typically uniform from leading to trailing edge on the blade's pressure side and a broad, gradually rising plateau of high pressure advanced in front of the blade.

The main features of the flow are marked on the figure. A pressure depression or basin (A) sat roughly 15% of chord aft of the leading edge and covered about 20% of the spacing from the blade suction side. The central region of this depression invariably included the lowest pressure in the whole passage distribution. Two pressure gulleys were also persistent features of the flow. Minimum pressure conditions at all axial stations corresponded to the gulley marked (B) on the surface. The gulley marked (C) ran diagonally across the passage from the blade suction-side leading edge toward the pressure side trailing edge. This diagonal (C) gulley was a *local* minimum in the otherwise monotonic pressure rise toward the pressure side of the passage. The pressure patterns and key features were found to be very repeatable from blades 1-2 to 2-3 to 3-4. This was consistent with the expected periodicity of the flow.

Computed blade-to-blade pressure contours were generated from a meridional throughflow calculation (Hirsch and Warzee, 1979) for the flow in the second rotor at the wall under design flow conditions. Major differences between the measured and computed pressures occur in Figure 4 *on the suction side* at the tip, as follows; (a) the low pressure basin formation and its position well aft of the leading edge is not predicted in the inviscid solution, (b) the low pressure gulleys which show as local bulges in the measured pattern are not calculated and (c) the minimum pressure location, which lies centrally in the basin, is calculated to lie very close to the suction side on the leading edge. Otherwise, there is a general correspondence in the patterns. The divergence of the pressure patterns along the suction side of the blade reflects the presence of the wall motion, the clearance gap and the inflow skew.

Change in Pressure Basin with Flow Coefficient Figure 5 shows that the low pressure basin changed its shape with a change in flow coefficient but always included the 25% axial chord station. It elongated, extending toward the leading edge at the low flow and extended aft, further away from the blade and became shallower as flow coefficient was increased.

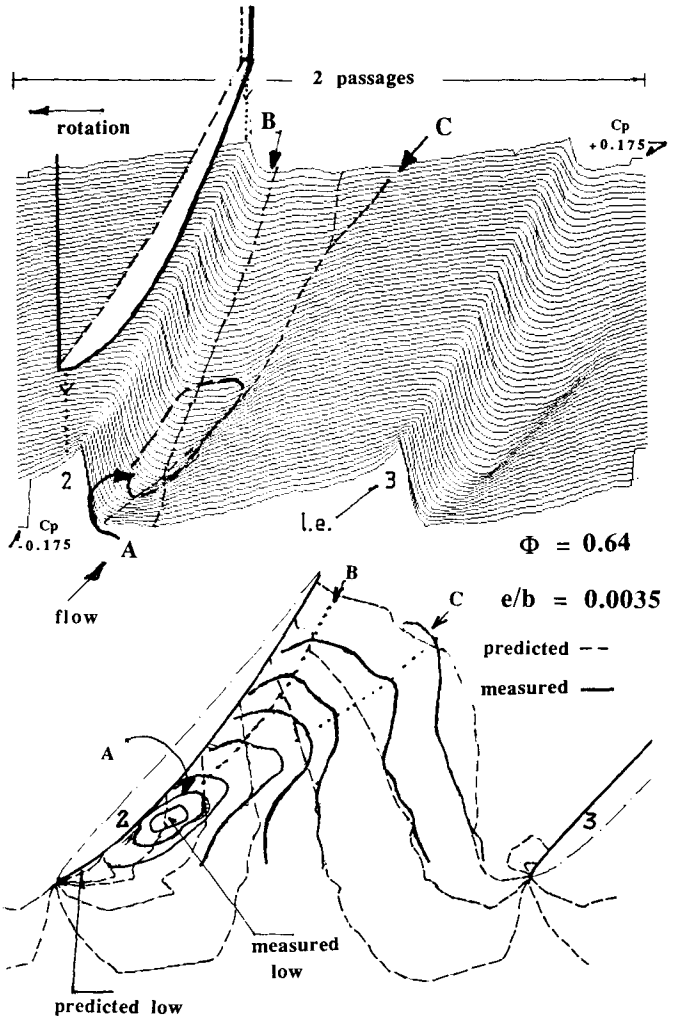

Fig. 4 (a) Surface plot of the pressure distribution on the annulus wall and the corresponding contour plot overlayed with computed contours.

Downloaded From: https://proceedings.asmedigitalcollection.asme.org on 04/08/2019 Terms of Use: http://www.asme.org/about-asme/terms-of-use

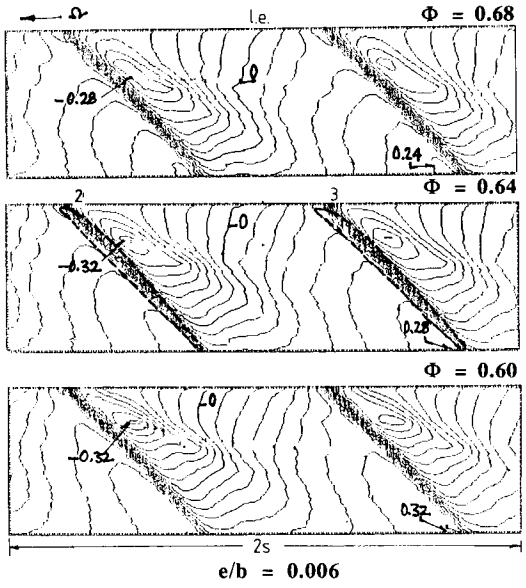

Fig. 5 Wall pressure contours (e/b = 0.006, *stator average*) for three flow conditions, (top) open throttle, (mid) design flow and (bot) near peak power.

Behavior of the Pressure Minimum (Gulleys) In Pattern The two low pressure depressions (or gulleys), which were noted in the pressure pattern, behaved differently with changing flow conditions. The minimum depression gulley (B), which stood off the blade suction side and ran the length of the blade roughly parallel to the chord, did not change its position with flow coefficient. The other low pressure gulley (C), running diagonally across the passage tended to move slightly closer to and swing toward the blade suction side as flow coefficient increased. It should be noted that the region between these two lines of low pressure formed a higher pressure region with a wedge like shape extending from a broad base near the trailing edge to a point immediately downstream of the low pressure basin. This wedge appeared as a distinct saddle (low-high-low) at the downstream end of the pressure basin when viewed on an oscilloscope.

Lowest Pressure Displaced from Suction Side The *location* of the blade-to-blade pressure minimum gulley (B) at all axial stations was a significant aspect of the flow pattern. While the position of the *maximum pressure ridge* in passage 1-2 was close to the blade pressure side edge, the *minimum pressure gulley* lay well away from the suction side blade surface in passage 2-3. The circumferential distance from maximum to minimum was much larger than the corresponding distance between the intervening blade surfaces. The spacing of peak-to-peak pressure exceeding the blade thickness was also observed by Heinemann (1985) in a turbine rotor. As boundary layers are thinner in turbines, the present spacing did not seem attributable to the presence of compressor boundary layers.

Wall Shear Correlation with Wall Pressure Figure 6 shows the wall shear levels at the second and fifth axial station in passage. The second axial station coincided with the position of the low pressure basin (A) on the blade's suction side. The shear measurements at this station indicated that the absolute flow was stagnant in the interval between the blade suction side and the minimum pressure gulley (B) running outboard of the suction side. In the relative frame this was equivalent to flow passing under the blade at wall speed and continuing at that velocity for a distance into the passage. Wall shear measurements in the passage at the fifth axial station had the same form, however, the shear level began to increase closer to the blade. This indicated that the relative flow decelerated from wall speed closer to the suction surface near the trailing edge.

If the velocity under the tip is estimated from the pressure difference across the blade using an inviscid analysis, the gap velocity should be large along the forward part of the blade and smaller near the trailing part. The shear measurements, however, showed that the relative flow moved at wall speed under the blade along its length. This suggested *pressure driven leakage was not the dominant factor in the flow and viscous effects were significant.* The location of minimum pressure gulley (B) appeared to be due to the wall dragging low energy fluid away from the suction side at wall speed or, alternately, the absence of passage throughflow penetrating into the corner at the tip aft of the peak suction basin. The measurements indicated this viscous region of flow moved with the blade.

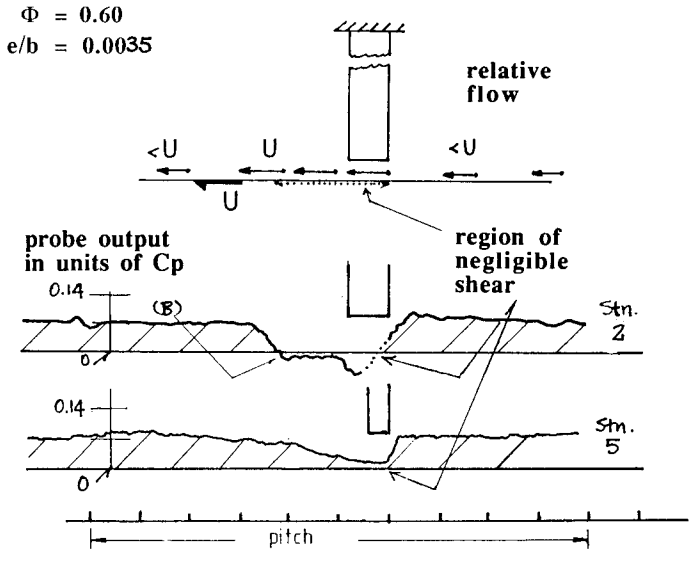

Fig. 6 Measured shear at the wall in the tangential direction at two axial stations. The regions of negligible shear indicate relative flow at wall speed and lie under the tip and outboard of the suction edge.

Downloaded From: https://proceedings.asmedigitalcollection.asme.org on 04/08/2019 Terms of Use: http://www.asme.org/about-asme/terms-of-use

Composite Flow Structure From consideration of both the wall pressure and the shear data, two flow processes seemed to determine the flow structure at the tip *for the small clearance conditions* measured. The first was a low pressure (higher velocity) region originating at the blade leading edge corner, or at the end of a separation lying in the corner, which crossed the passage (path C of Fig. 4). Its direction was only slightly dependent on the stage's mean line incidence in the forward part of the passage. With downstream convection the direction and strength of this cross passage formation varied more with meanline incidence. This process appeared to be a vortical filament some distance above path C rolling up flow near the wall. The second process created a fillet-like region of relatively higher static pressure fluid in the suction surface-to-wall corner. This fillet had a distinct footprint on the wall outboard of the suction side and resembled an extension the blade surface to the line of minimum pressure some distance off the blade. The two regions of flow motion coalesced or converged and appeared to form the low pressure basin, which stood off the suction surface downstream of the leading edge. The main features of the tip flow are shown schematically in Figure 7.

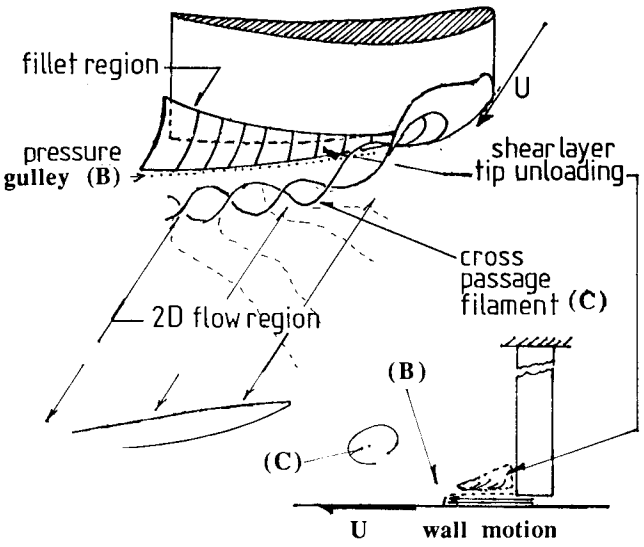

Fig. 7 Schematic of main features of the flow at the tip on the suction side of the passage.

CHANGE OF TIP FLOW STRUCTURE WITH CLEARANCE VARIATION

The effect of tip clearance changes on the flow were explored by observing changes in the wall pressure patterns. Comparisons were made at the same flow coefficient for either the same stator relative location of the probe or for the averaged flow. Results from the design flow condition, shown in this paper, were similar to the other flow conditions.

Change in Pressure Pattern (Stator Averaged) Figure 8 shows the result of *subtracting* the *stator averaged* pressure pattern of one clearance level from another. The pressure only changed in a very abrupt, uniform band of increased pressure (unloading) along the blade tip. The uniformity was consistent with a relative velocity of wall speed under the blade along the tip. A diffuse lowering of the wall pressure was barely noticeable crossing the passage. The slightly lowered pressure occurred along C of Fig. 4. The relative strength of the two effects suggested that the tip-to-wall corner unloading was not appearing as increased vorticity in the cross passage direction *close* to the wall.

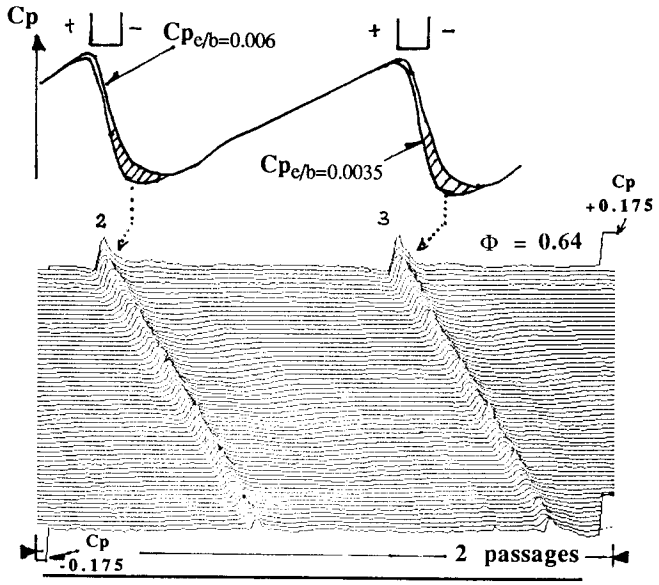

Fig. 8 Surface plot of the *difference* in *stator averaged* wall pressure *due to a change of clearance* in the rotor (pressure of e/b = 0.006 clearance minus pressure of e/b = 0.0035 clearance), at the design flow.

Change in Pressure Pattern (Stator Relative) Figure 9 shows changes in the pressure contours, at the same flow and *stator relative circumferential location* of the probe, for different clearance levels. The changes with increasing clearance show a progressive unloading at the suction surface-to-wall corner and an increasing zone of depression (D) extending diagonally rearward in the passage. The form of this depression was dependent on the stator relative location and its changes were not significant on a stator averaged basis. The tip unloading, however, was present at all stator relative locations.

Blade Surface Pressure Unloading Changes in blade pressure distribution and tangential loading, based on wall pressures as a function of axial position, are shown in Figure 10 for three clearances. As the clearance enlarged, the following were noted: (a) The pressure-side and pressure levels did not change significantly while the pressure on the suction-side increased noticeably. However, the lowest pressure magnitude in the passage remained almost constant. (b) The circumferential spacing between the maximum (ridge) and minimum pressure

Downloaded From: https://proceedings.asmedigitalcollection.asme.org on 04/08/2019 Terms of Use: http://www.asme.org/about-asme/terms-of-use

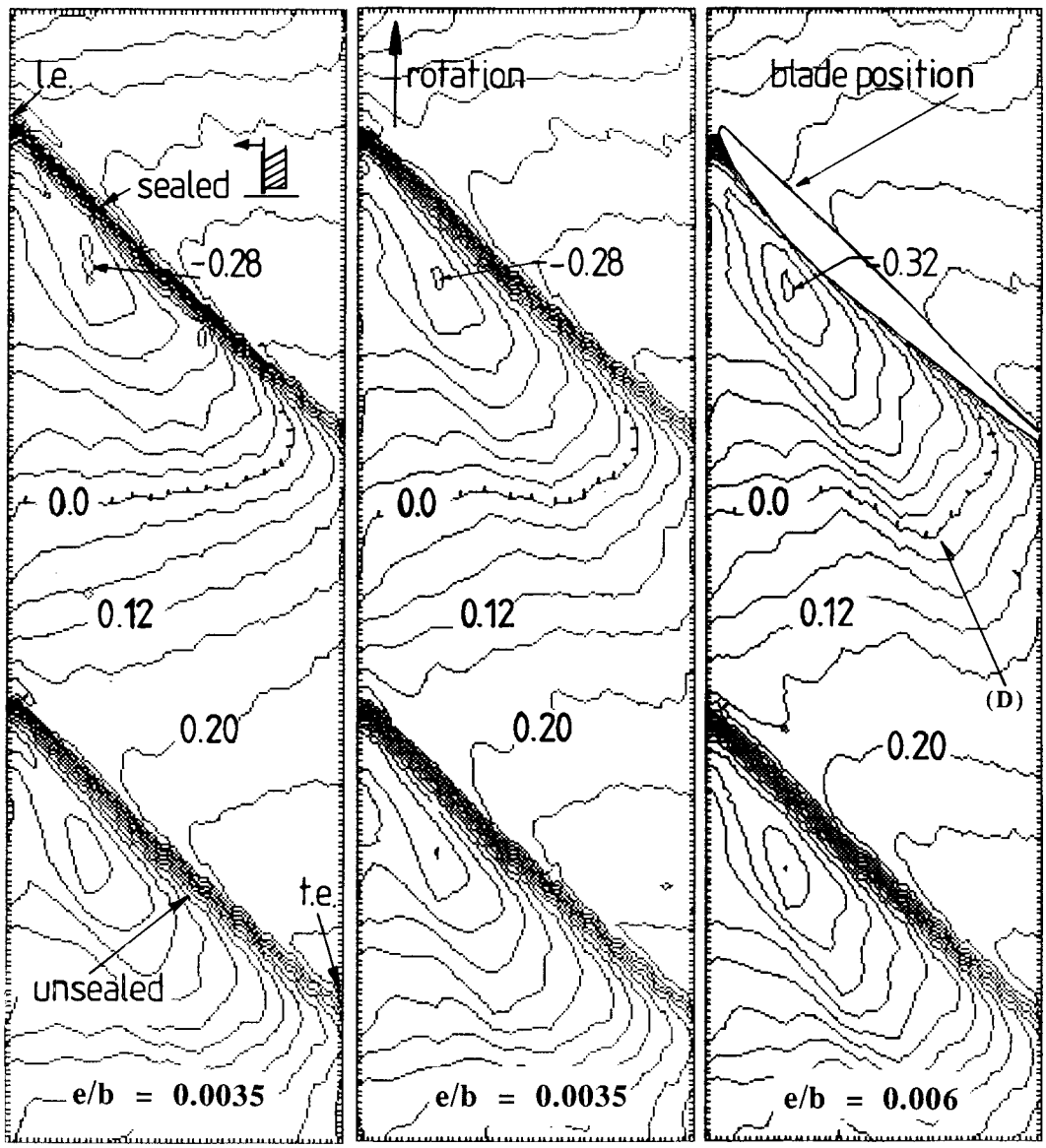

Fig. 9 Wall pressure contours *at stator relative location 3* for three clearances, (left) sealed tip on blade 2, (mid) e/b = 0.0035 clearance and (right) e/b = 0.006 clearance for the design flow.

(gulley) on either side of the blade remained unchanged but the position of the features moved slightly in the direction of wall relative motion for the larger clearance.

Invariant Features of the Flow Changes in pressure distribution and loading *due to a clearance change* were essentially the same at other flow coefficients. This suggested the stage's mean line incidence, which varied from -1.25° to +3.5°, had minimal influence on the tip flow near the blade surfaces. The average pressure patterns also showed that the pressure basin location and its general shape and orientation in the passage changed minimally. Similarly, the position of the abrupt pressure rise on the pressure side of the basin showed minimal change for the small clearance changes tested. However, the position of the abrupt pressure rise moved slightly with stator relative position. This slight movement resulted in very large pressure fluctuations occurring in a narrow zone well out in the passage. The position of this movement of the abrupt pressure rise is consistent with the location of a zone of high turbulence intensity measured by Lakshminarayana et al. (1982, Fig. 8) in a rotor passage. A similarly shaped zone in the present rotor was seen in contour plots of pressure fluctuations from the stator average.

Downloaded From: https://proceedings.asmedigitalcollection.asme.org on 04/08/2019 Terms of Use: http://www.asme.org/about-asme/terms-of-use

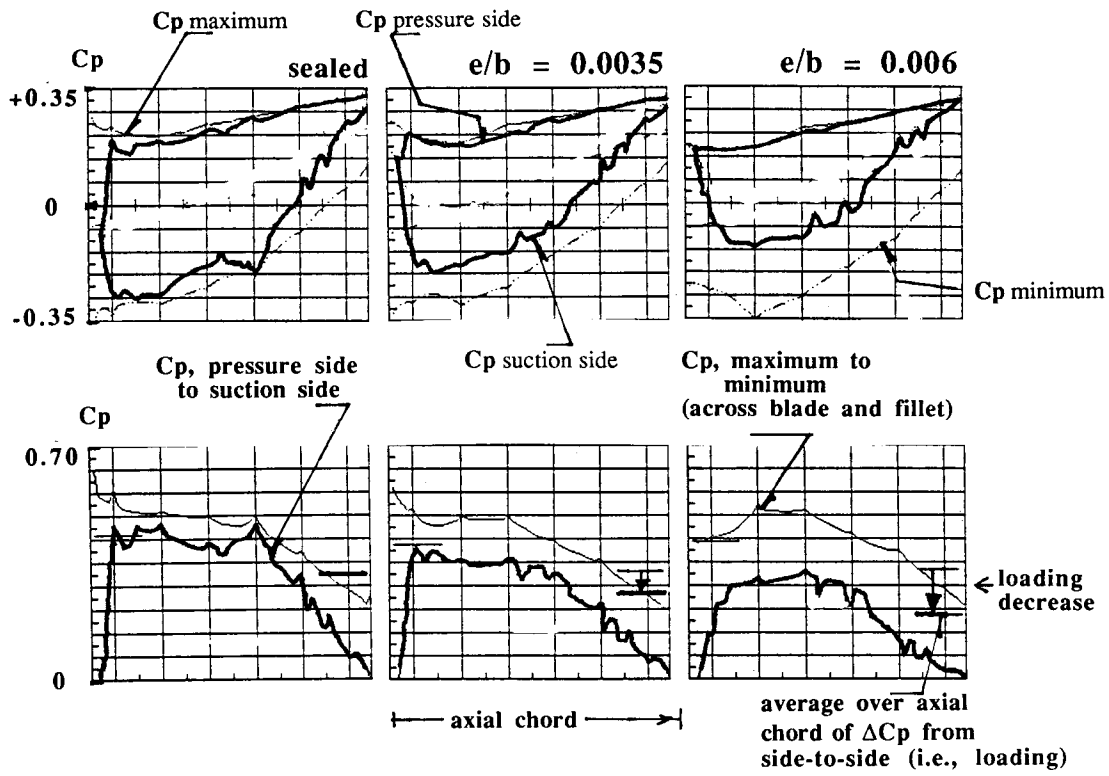

Fig. 10 Tip pressure distribution and loading as function of axial position *at stator relative location 3* for three clearances, (left) sealed tip on blade 2, (mid) e/b = 0.0035 clearance and (right) e/b = 0.006 clearance for the design flow.

DISCUSSION

The present measurements were made in the second stage of a multistage compressor. If the wall pressures are compared to those measured by Inoue and Kuroumaru (1988) in an isolated rotor, the displacement of the path of the minimum pressure gulley away from the tip suction surface is much larger in the present case. Relative flows at wall speed near the suction side are observed in both cases, however, in the present rotor the region of wall speed extends further forward along the suction surface. The differences generally support the analysis of Moyle (1989a), which proposed that the tip local flow in Inoue's stage would not be the same as the present stage due to the different ratios of wall shear to centrifugal forces found in the two compressors. In the present study it was also noticeable that the peak suction level for the passage remained constant, in absolute pressure magnitude, over the range of flow coefficients tested and changed only slightly with clearance. In absolute magnitude, the pressure on the pressure side near the tip rose with decreased throughflow to produce higher blade loading rather than increased incidence producing higher velocity on the suction side. Consequently, the displacement of the minimum pressure gulley into the passage and the flow moving at wall speed in the region between the suction surface and minimum pressure gulley changed little with flow coefficient.

Recent measurements by Storer and Cumpsty (1990) in a linear cascade provide very detailed wall pressure surveys near a tip gap which permit a comparison of a cascade tip flow to the present rotor tip flow. Their measurements show the minimum pressure lying along the blade suction surface, consistent with the cascade not having wall motion and inflow skew. Unlike their results, the blade tangential loading decreased at the tip with increased clearance in the present rotor (Fig.10). As discussed previously, the relative flow issuing into the passage along the length of the tip gap moved at wall speed under the rotor tip. There was no evidence of the

Downloaded From: https://proceedings.asmedigitalcollection.asme.org on 04/08/2019 Terms of Use: http://www.asme.org/about-asme/terms-of-use

leakage velocity correlating with the blade pressure loading as was found in their cascade. The sharp peaking of the blade loading near mid chord that occurred in the cascade with an increase in clearance from 2 to 4% of chord could not be directly compared with the changes from 0.8 to 1.35% of chord in this compressor, however, it was clear that the compressor's tangential loading was more even along the blade and decreased evenly with the clearance increases tested. Storer and Cumpsty emphasized that an intense shearing in a thin layer between the leakage flow issuing into the passage and the passage throughflow was the principal mechanism for the high loss associated with tip leakage in the cascade. This layer has also been discussed by Inoue and Kuroumaru in interpreting their measurements. Such a layer was also implied by the present measurements and its thickness was determined, in Moyle (1989b), to be 0.20 of gap height compared to 0.13 in the cascade.

In the present data, the close agreement between the peak-to-peak pressure difference (wall maximum to minimum) along the rotor tip with the computed blade loading is noteworthy. Although the minimum pressure did not lie at the suction side of the blade, the closeness of the axial distributions of maximum to minimum pressure to the inviscid pressure predictions for the blading suggested the predicted flow velocities occurred further out in the passage. This situation was not altered by changing clearance.

CONCLUSION

The major observations are summarized as follows:

(1) The most remarkable feature of the flow structure was the path of the minimum suction pressure in the passage. Rather than coinciding with the suction surface, the minimum pressure gulley at all axial stations in the passage was displaced approximately twice the blade maximum thickness away from the blade suction surface. The peak suction pressure in the passage also remained roughly constant over the range of conditions tested. These observations strongly suggested a viscous or shearing layer was generated on the blade side of the tip gap which modified the inviscid relative flow field and produced an unloading on the blade tip. This is in contrast to the situation in a stationary cascade where loading was restored with the presence of a clearance.

(2) The consequence of changing the clearance from a sealed tip to small gaps (e/b = 0.0035 and e/b = 0.006) was to progressively and uniformly unload the blade tip while maintaining an almost constant pressure difference from maximum to minimum wall pressure across the tip and viscous region. In concert with the tip unloading, a slight decrease in pressure occurred along the cross passage minimum pressure gulley.

The fundamental flow structure at the wall (i.e., the minimum pressure gulley, the cross passage vortex filament path and their resulting basin) appeared to be generated by the blade motion relative to the wall. Changes in mean line incidence of the stage, stator relative position and tip clearance gap appeared to interact with this basic structure but not cause any fundamental change in its character.

Acknowledgements

This work was supported as part of a tip clearance study at the Naval Postgraduate School by the Naval Air Systems Command, Air Breathing Propulsion Research Program under the cognizance of G. Derderian.

References

Heinemann, H-J., (1985) "High Speed Data Acquisition and Reduction for Wall Static Pressures within the Passage of a Rotating Annular Turbine Cascade," Eighth Symposium on Measuring Techniques for Transonic and Supersonic Flows in Cascades and Turbomachines, Universita Degli Studi Di Genova.

Hirsch, C. and Warzee, G., (1979) "An Integral Quasi-3D Finite Element Calculation Program for Turbomachinery Flow," ASME Journal for Engineering for Power, Vol. 101, pp. 141-148.

Inoue, M. and Kuroumaru, M., (1988) "Structure of Tip Clearance Flow in an Isolated Axial Compressor Rotor," ASME 88-GT-251.

Lakshminarayana, B., Pouagare, M. and Davino, R. (1982) "Three Dimensional Flow Field in the Tip Region of a Compressor Rotor Passage - Part II, Turbulence Properties," ASME 82-GT-234.

Moyle, I. N., (1989a) "Influence of the Radial Component of Total Pressure Gradient on Tip Clearance Secondary Flows in Axial Compressors," ASME 89-GT-19.

Moyle, I. N., (1989b) "Tip Clearance Effects in Axial Flow Compressors - An Experimental and Analytical Study," PhD Dissertation, University of Tasmania and also Naval Postgraduate School, California, NPSAA91-001CR.

Storer, J. A. and Cumpsty, N. A., (1990) "Tip Leakage Flow in Axial Compressors," ASME 90-GT-127.

Vavra, M. H., (1973) "Aerodynamic Design of Symmetrical Blading for a Three-Stage Axial Flow Compressor Test Rig, " Naval Postgraduate School, Monterey, California, NPS-57-Va73121A

Downloaded From: https://proceedings.asmedigitalcollection.asme.org on 04/08/2019 Terms of Use: http://www.asme.org/about-asme/terms-of-use